CARMENES as an Instrument for Exoplanet Research

José A. Caballero
Centro de Astrobiología, CSIC-INTA, ESAC Campus, Camino Bajo del Castillo s/n, 28692 Villanueva de la Cañada, Madrid, Spain
e-mail: caballero@cab.inta-csic.es

Walter Seifert, Andreas Quirrenbach
Landessternwarte, Zentrum für Astronomie der Universität Heidelberg, Königstuhl 12, 69117 Heidelberg, Germany
e-mails: aquirren@lsw.uni-heidelberg.de, w.seifert@lsw.uni-heidelberg.de

Pedro J. Amado
Instituto de Astrofísica de Andalucía (IAA-CSIC), Glorieta de la Astronomía s/n, 18008 Granada, Spain
e-mail: pja@iaa.es

Ignasi Ribas
Institut de Ciències de l'Espai (ICE, CSIC), Campus UAB, c/ Can Magrans s/n, 08193 Bellaterra, Barcelona, Spain and Institut d'Estudis Espacials de Catalunya (IEEC), c/ Gran Capità 2–4, 08034 Barcelona, Spain
e-mail: iribas@ice.csic.es

Ansgar Reiners
Institut für Astrophysik und Geophysik, Georg-August-Universität, Friedrich-Hund-Platz 1, 37077 Göttingen, Germany
e-mail: ansgar.reiners@phys.uni-goettingen.de

To be published in: Handbook of Exoplanets, 2nd edition, Hans Deeg and Juan Antonio Belmonte (eds. in chief), Springer International Publishing AG, part of Springer Nature

Fig. 1 Dome and building of the 3.5 m Zeiss telescope at Calar Alto on a snowy day during CARMENES assembly — Winter 2015-2016. Credit: CARMENES.

Fig. 2 The CARMENES logo. “solmirobauhaus” is the Spanish “Sol de Miró” as if it had been revisited by the German Bauhaus — Fall 2009. The logo is the 21st-century fusion of two very Spanish and German concepts. CARMENES was also the first astronomical instrument to have a soundtrack (listen to it in Antonio Arias’ album *Multiverso II*). Credit: CARMENES.

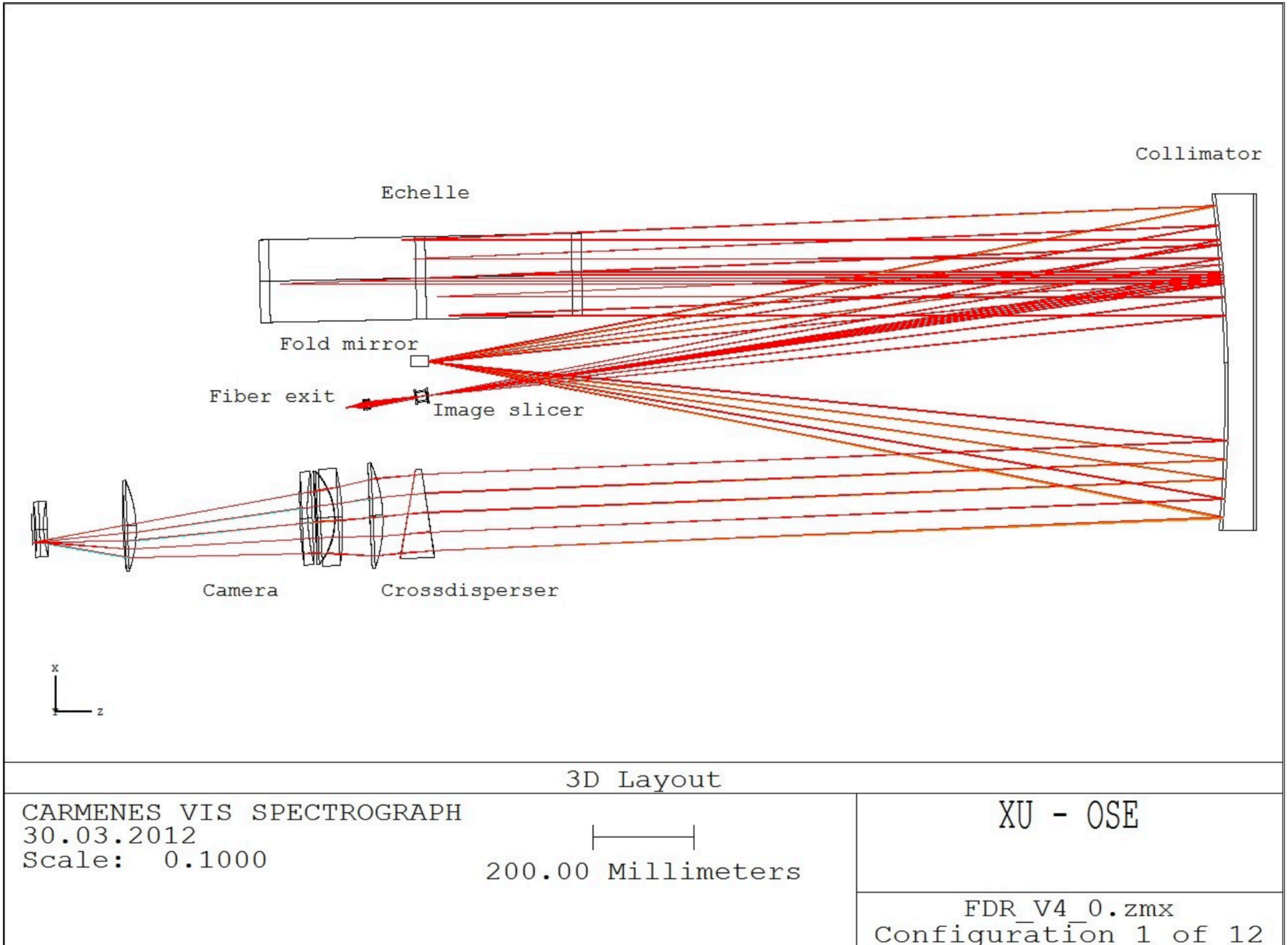

Fig. 3 The CARMENES VIS channel optical layout — Spring 2012. The NIR one is very similar. Credit: CARMENES.

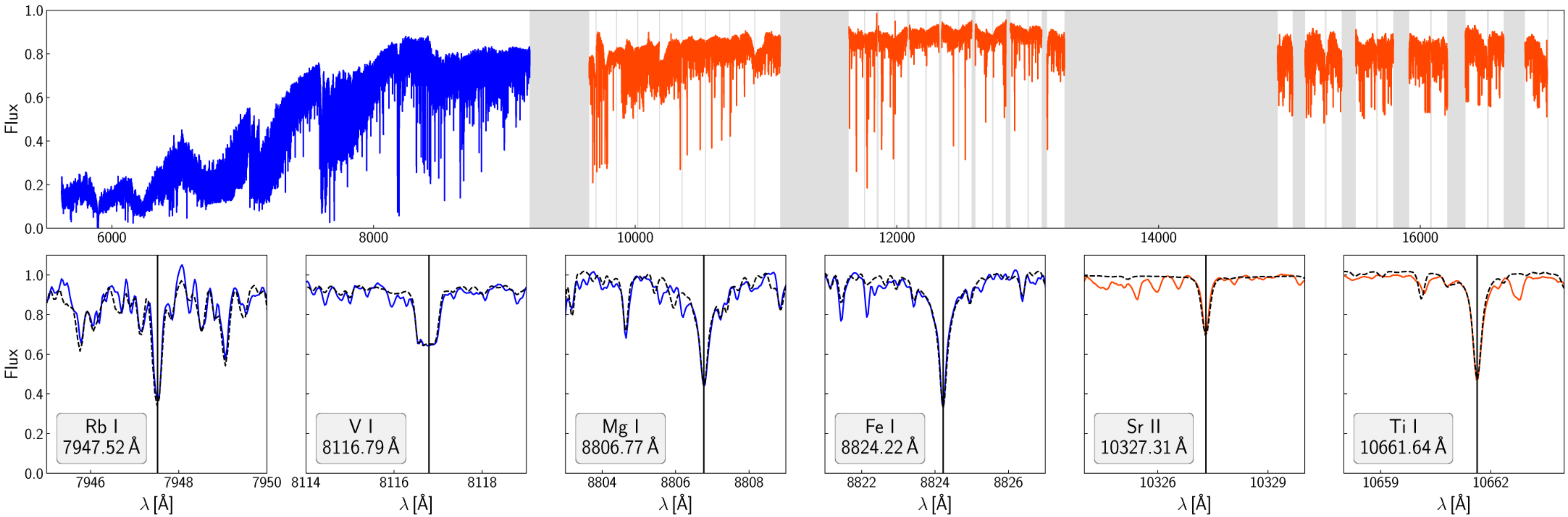

Fig. 4 The CARMENES wavelength coverage. *Top panel:* coadded, order-merged, channel-merged CARMENES VIS (blue) and NIR (red) template spectrum of exoplanet-host M3.5 V-type star GJ 486. Interruptions (grey areas) are due to strong telluric contamination and inter-order and NIR detector array gaps. *Bottom panels:* zoomed-in view of six representative, weakly magnetic-sensitive atomic lines. Black dashed lines are synthetic fits. Credit: CARMENES, adapted from Caballero et al. (2022).

Fig. 5 Installation of the CARMENES front-end at the Cassegrain focus of the 3.5 m Calar Alto telescope — Spring 2015. The light blue box and golden cylinders are the PMAS electronics and detector cryostats. Credit: CARMENES.

Fig. 6 Transportation of the wrapped CARMENES NIR channel tank inside the 3.5 m telescope building to its final location in the coudé room — Summer 2015. This was one of the scariest moments of the project, as the NIR tank contained during transportation the optical bench and some opto-mechanical mounts, unlike the VIS channel. The tough decision ended up being the right one. Credit: CARMENES.

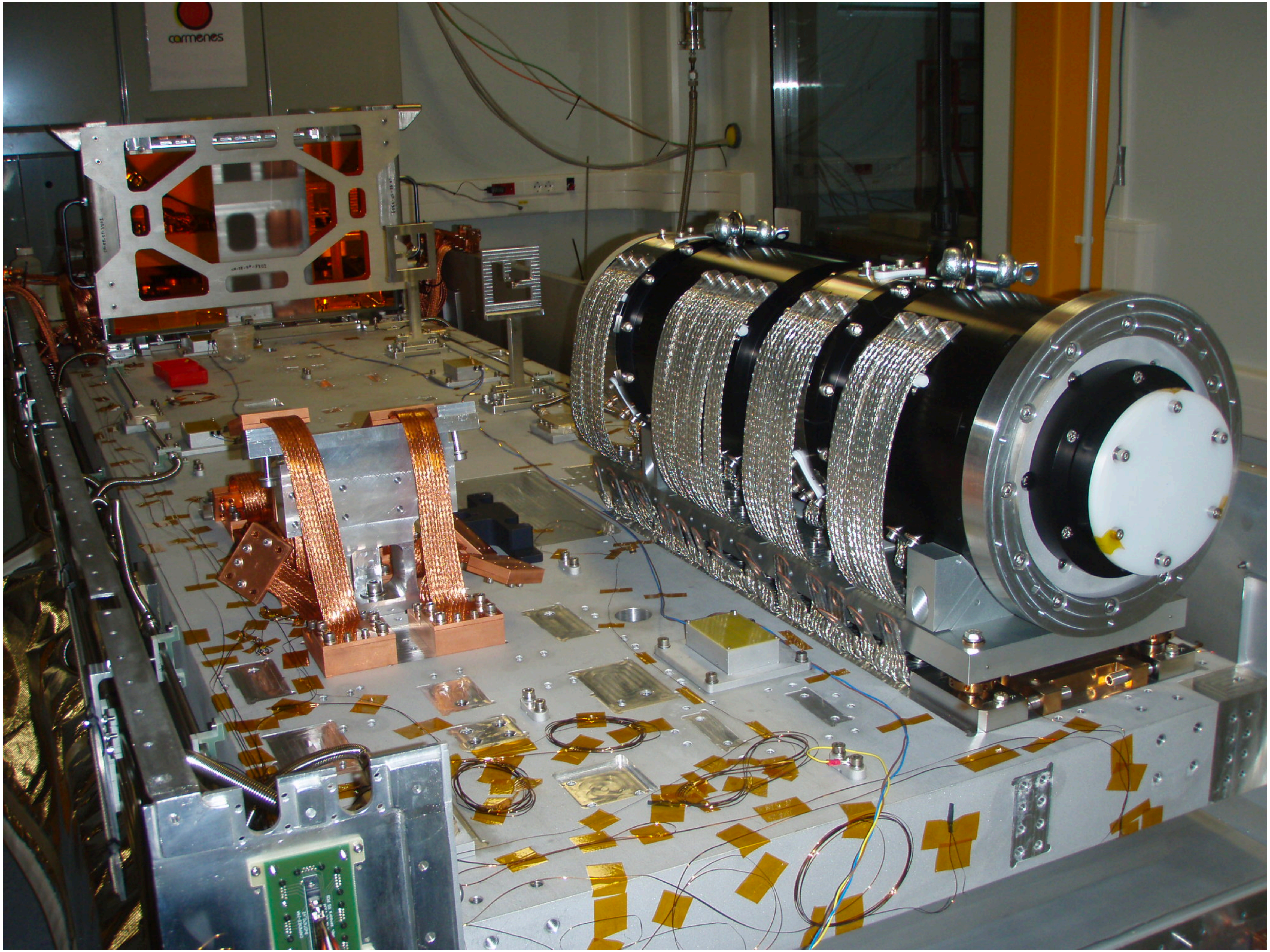

Fig. 7 NIR optical bench after installing the camera, mounts of the collimator mirror and échelle grating, lower part of the radiation shield, and a number of temperature sensors (attached with kapton tape) — Summer 2015. The VIS optical bench is similar. Credit: CARMENES.

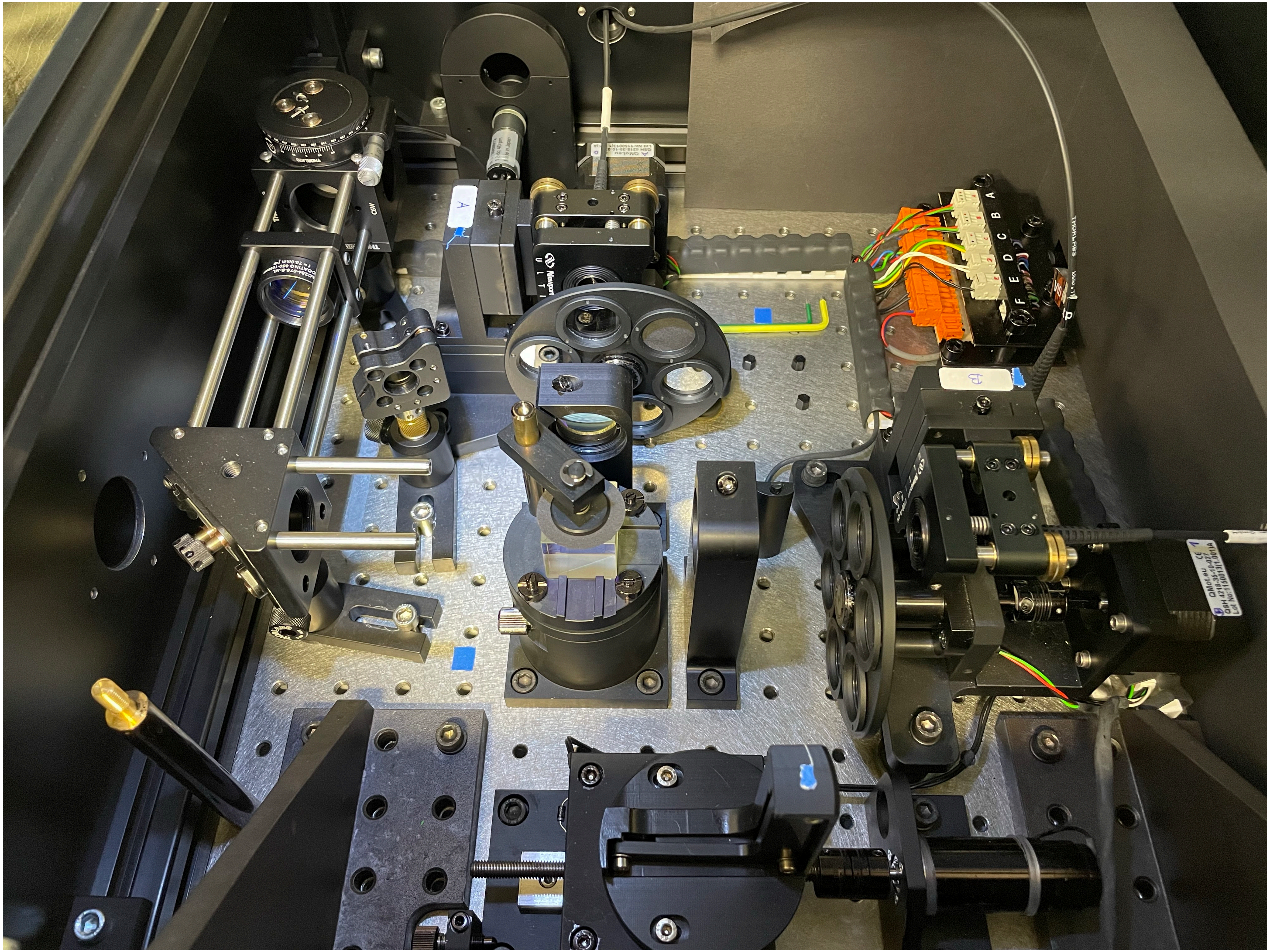

Fig. 8 NIR calibration unit optical bench after the Fabry-Pérot etalon — Spring 2024. Credit: CARMENES.

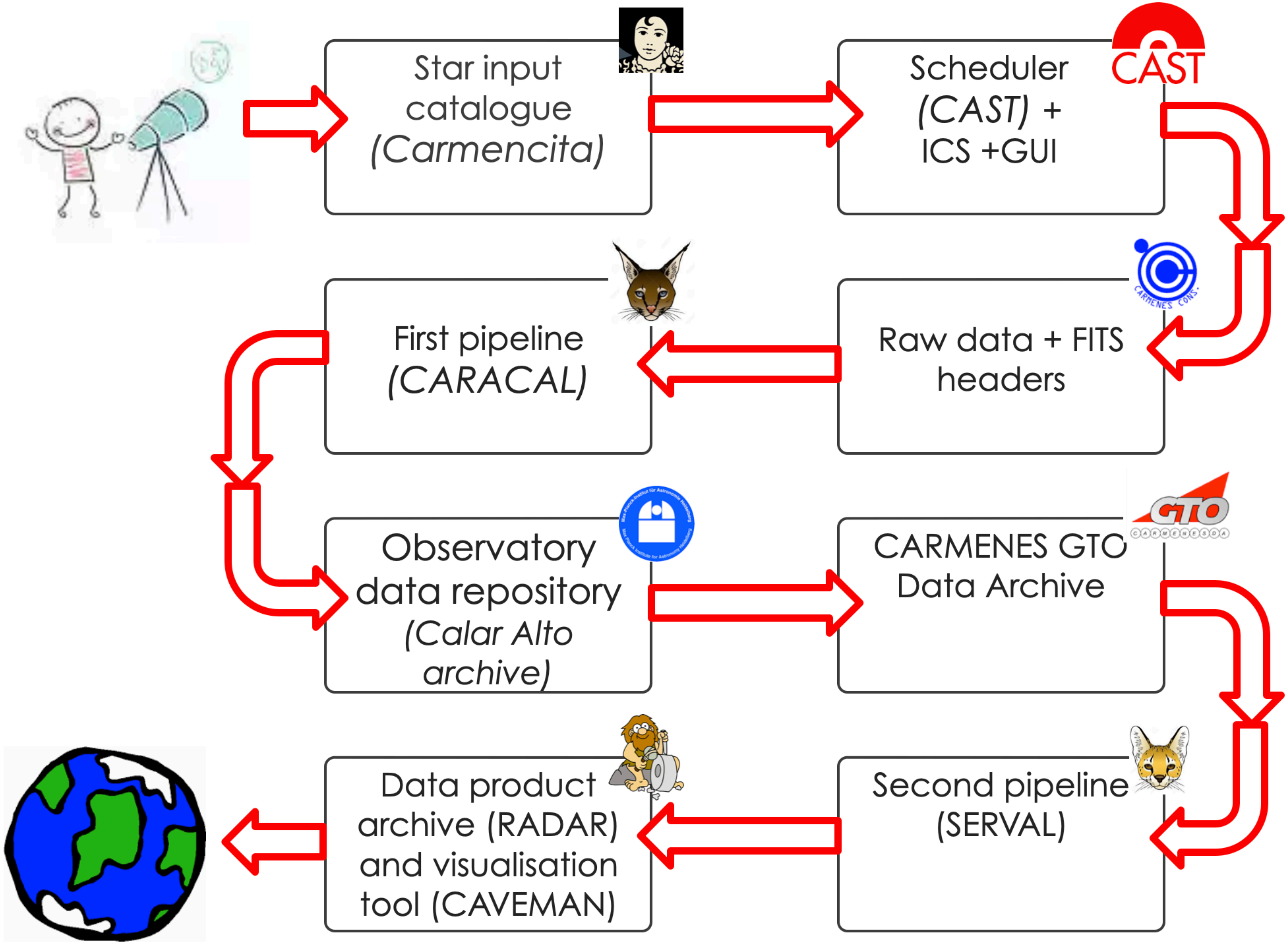

Fig. 9 The whole CARMENES data flow from the astronomer to the exoearth. Credit: CARMENES, adapted from Caballero et al. (2016b).

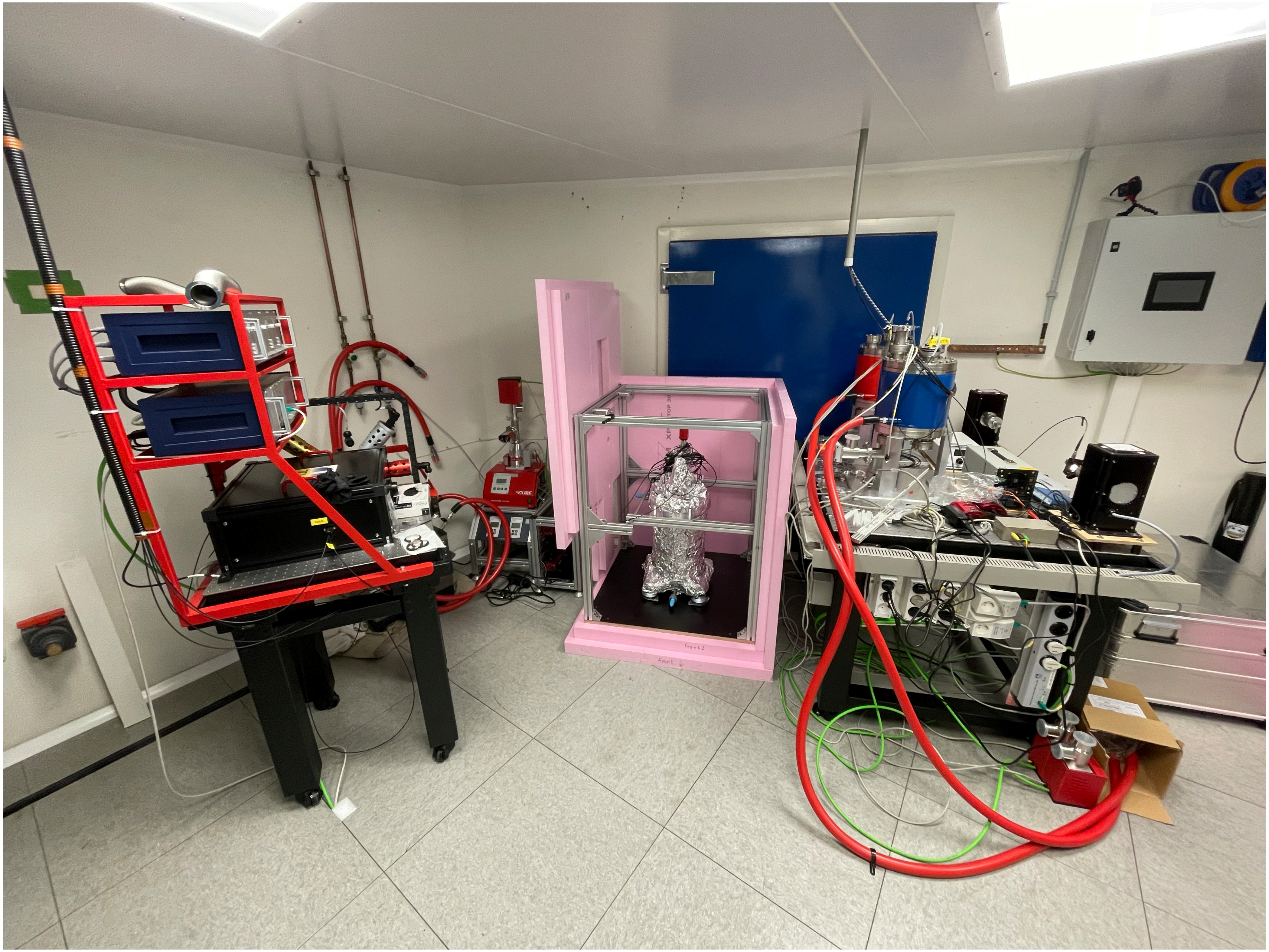

Fig. 10 Installation of the new joint VIS+NIR Fabry-Pérot etalon cryostat inside the 3.5m telescope calibration room — Spring 2024. From left to right: the NIR calibration unit (partly rotated, red), silicone oil pump (cornered, partly visible), vaccum pump (cornered, red), new Fabry-Pérot cryostat (wrapped in aluminium and inside an isolated box, dubbed “Barbie”) and optical bench with decommissioned VIS (blue) and NIR (red) Fabry-Pérot cryostats and halogen lamps (black). The VIS calibration unit and super-master-lamp storage tank are out of the image to the left and right, respectively. Credit: CARMENES.

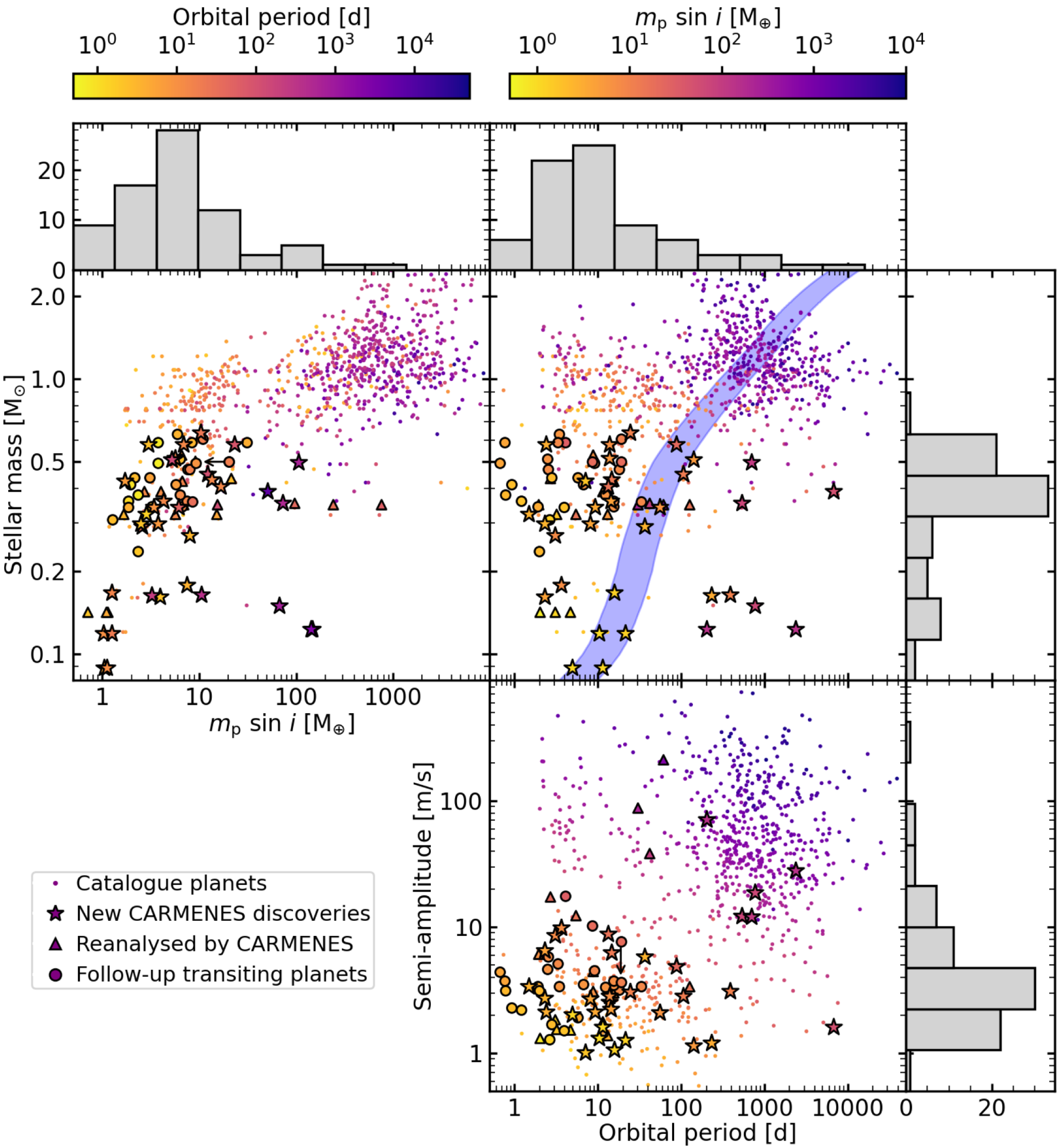

Fig. 11 Scatter plots of the CARMENES first data release exoplanet sample compared to the complete sample of catalogued planets in the NASA Exoplanet Archive detected via RVs (903; small dots). Different symbols indicate planets newly detected from the CARMENES blind survey (33; stars), planets confirmed from transit follow-up (26; circles), and known planets re-analysed with CARMENES data (17; triangles). The three panels correspond to pairs of different relevant parameters, with the complementary colour scale introducing a third dimension. The histograms along the axes show distributions of the corresponding parameters for the CARMENES planet sample. The blue shaded band in the top-right panel represents the liquid-water habitable zone with limits defined by the 'runaway greenhouse' and 'maximum greenhouse' criteria. Credit: CARMENES, adapted from Ribas et al. (2023).

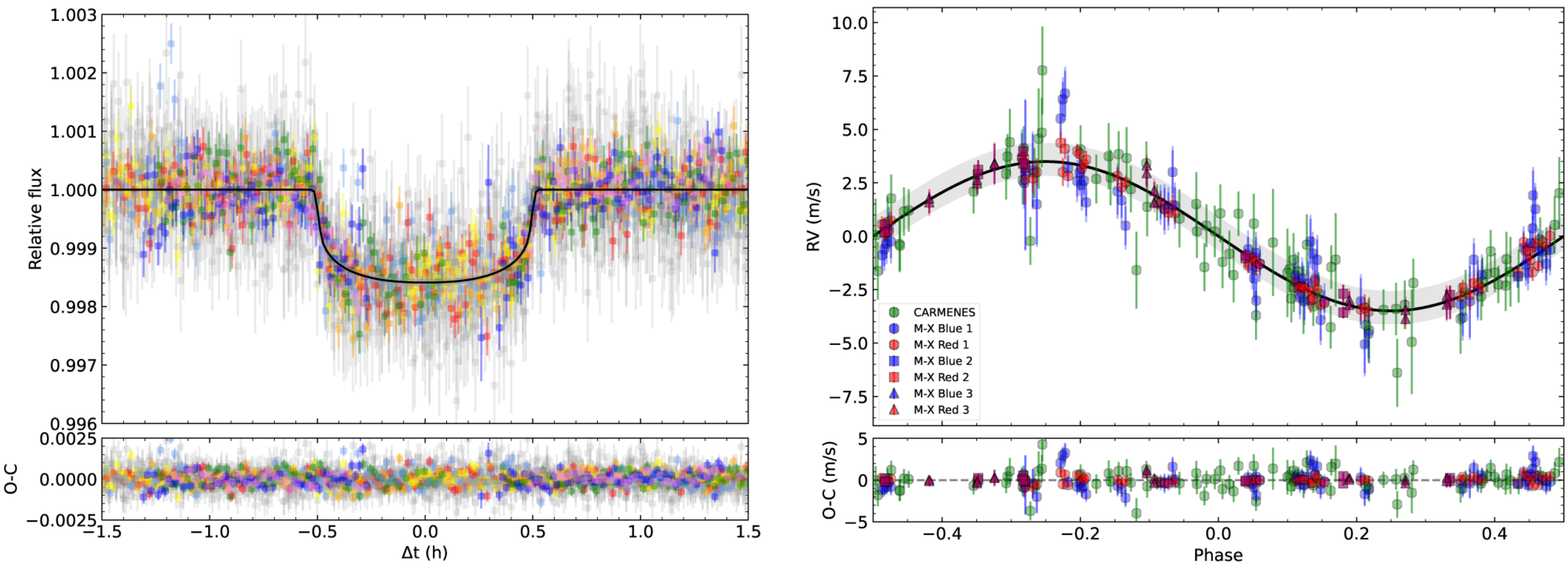

Fig. 12 Phase-folded transit and RV data and one-planet+Gaussian-process model fits. *Left:* light-curve model fit (black line) and CHEOPS+TESS data (CHEOPS transit #1: red, #2: orange, #3: yellow, #4: green, #5: light blue, #6: dark blue, #7: pink, and TESS: grey). *Right:* RV-curve model fit (black line with $\pm 1\sigma$ uncertainty marked with a grey shaded area) and CARMENES+MAROON-X data (CARMENES: green circles, MAROON-X Red: red symbols, and MAROON-X Blue: blue symbols. MAROON-X data are split into runs 1 [circles], 2 [squares], and 3 [triangles]). Error bars include original RV uncertainties (opaque) and jitter added in quadrature (semi-transparent). Credit: CARMENES, adapted from Caballero et al. (2022).

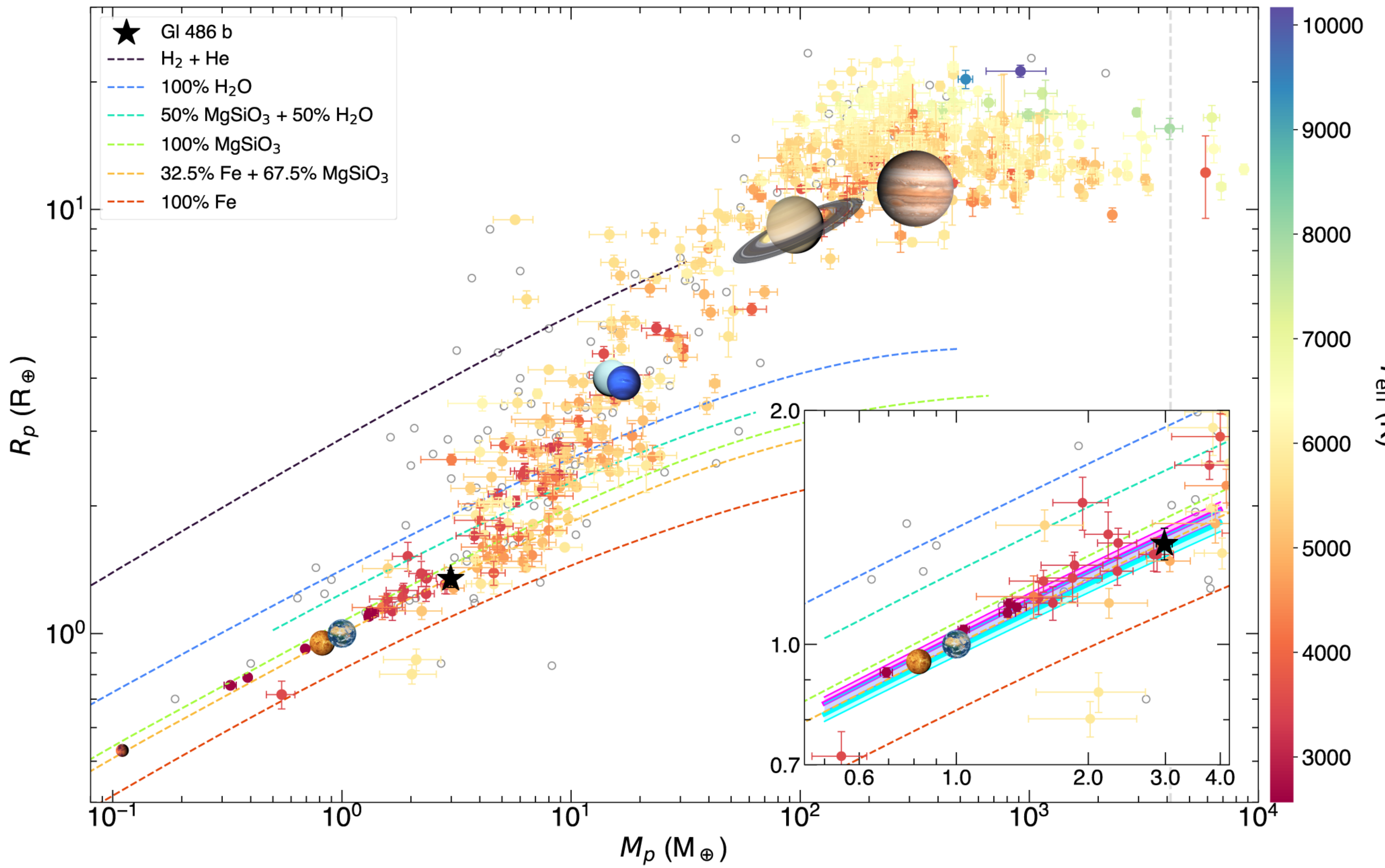

Fig. 13 Mass-radius diagram of all transiting exoplanets with mass determination (from RV or transit time variations) known in 2022, in comparison with the Solar System planets. Filled circles with error bars colour-coded by their host's T_{eff} are planets with mass and radius uncertainties of less than 30%, and open grey circles are the others. The filled black star is Gl 486 b. Dashed coloured curves are theoretical models as specified in the legend. The Earth-like model is orange. The grey vertical dashed line is the deuterium burning mass limit at 13 M_{Jup} ('planet'-brown-dwarf boundary). In the inset, we zoom in around the smallest planets and add mass-radius relationships informed by stellar abundances. We plot median and 1σ error regions following nominal relative abundances of Fe, Mg, and Si of the host star without (pink) and with (cyan) an empirical correction based on well-characterised super-Earths. The two outliers with very high densities and $M \sim 2.0\ M_\oplus$ are Kepler-1972b and c, which are two transiting planets with masses determined from transit time variations. Credit: CARMENES, adapted from Caballero et al. (2022).